Ordered Phases in Aqueous Solutions of Diblock Oxyethylene/Oxybutylene Copolymers Investigated by Simultaneous Small-Angle X-ray Scattering and Rheology

J. A. Pople and I. W. Hamley*

School of Chemistry, University of Leeds, Leeds LS2 9JT, U.K.

J. P. A. Fairclough and A. J. Ryan

Manchester Materials Science Centre, Grosvenor Street, Manchester M1 7HS, U.K.

B. U. Komanschek and A. J. Gleeson

CLRC Daresbury Laboratory, Warrington WA4 4AD, U.K.

G.-E. Yu and C. Booth

Department of Chemistry, University of Manchester, Manchester M13 9PL, U.K.

Received March 6, 1997; Revised Manuscript Received July 8, 1997[⊗]

ABSTRACT: The phase behavior of gels of $E_{40}B_{10}$ in 0.2 mol dm^{-3} aqueous K_2SO_4 was studied as a function of temperature and concentration. $E_{40}B_{10}$ is a diblock copolymer of poly(oxyethylene) (E) and poly(oxybutylene) (B), where the subscripts denote the number of repeats. The phase of the material was characterized by both simultaneous rheology and small-angle X-ray scattering, (SAXS). Depending on polymer volume fraction in the range 23−38% a body-centered cubic (bcc) structure or a face-centered cubic (fcc) structure was observed at low temperature, and at high temperature a hexagonally packed rod structure was formed. The phase transitions were shown to be characterized by discontinuous changes in the values of the dynamic shear moduli. A bcc−fcc transition was observed at high concentration, the corresponding transition temperature increasing with increasing polymer concentration. The effects of reciprocating shear were shown to increase the degree of order, manifested as a sharpening of the diffraction peaks in the SAXS pattern. The dynamic moduli decreased rapidly on the application of oscillatory shear and recovered equally rapidly when the deformation ceased. The decrease in moduli was shown, via the SAXS patterns acquired simultaneously, to be correlated to structural changes within the gel.

Introduction

Solutions of block copolymers form interesting mesophases in which micelles pack into structures that vary with copolymer concentration and temperature. This study focuses on correlating rheological behavior with micellar structure for a range of aqueous solutions of a diblock copolymer $E_{40}B_{10}$ in a solution of 0.2 mol dm^{-3} aqueous K_2SO_4, where E denotes the hydrophilic oxyethylene unit OCH_2CH_2 and B denotes the hydrophobic oxybutylene unit $OCH_2CH(C_2H_5)$.

The self-assembly of copolymer $E_{40}B_{10}$ in dilute aqueous solution to form micelles follows the pattern reported for diblock E_mB_n copolymers in a series of earlier papers.[1−7] Given suitable compositions, spherical micelles with high association numbers and narrow size distributions are formed at low concentrations. As expected for a system with a negative temperature coefficient of solubility, the association number increases with increasing temperature. Addition of salt has a similar effect to raising temperature, in that the solvent becomes poorer. Indeed, 0.45 mol dm^{-3} K_2SO_4 at 35 °C is known to be a Θ solvent for poly(oxyethylene).[8,9] Examples of micellar association numbers and radii determined by light scattering methods for copolymer $E_{40}B_{10}$ in various aqueous solutions are given in Table 1.[1]

The gelation of aqueous micellar solutions of E_mB_n copolymers has been studied extensively as a function of temperature over the concentration range of the isotropic cubic phase[1−5,10] and recently over more extended concentration ranges.[11,12] A phase diagram covering the concentration range 20−40 wt % for copolymer $E_{40}B_{10}$ in 0.2 mol dm^{-3} K_2SO_4 is given in Figure 1, and forms the basis for the present experiments: to determine the structures underlying the range of observed phase behaviors. The notation "mobile" and "immobile" in this phase diagram refers to behavior in a tube inversion test, which is sensitive to yield stress and which, under the conditions used, assigns the classification "immobile" if the yield stress is significantly greater than 50 Pa.[11] The full symbols in Figure 1 were obtained in this way, and by visual observation of clouding. The open symbols relate to rheological properties, which are described below.

The most extensively investigated block copolyethers are the triblock copolymers $E_mP_nE_m$ (where P denotes oxypropylene), known commercially by their trade names: Pluronic polyols (BASF Corp.) or Synperonic PE

Table 1. Micellar Parameters for $E_{40}B_{10}$ in Aqueous K_2SO_4

K_2SO_4/mol dm^{-3}	T/°C	N_w[a]	r_t/nm[b]	r_h/nm[c]
0	20	23	4.0	8.5
0.2	20	32	4.6	8.9
0.4	20	45	5.0	7.8
0.4	30	55	5.2	7.5
0.4	45	80	4.6	7.6

[a] N_w, mass-average association number. [b] r_t, thermodynamic radius = equivalent hard-sphere radius. [c] r_h, hydrodynamic radius.

* Author to whom correspondence should be addressed.

[⊗] Abstract published in *Advance ACS Abstracts,* September 1, 1997.

S0024-9297(97)00308-2 CCC: $14.00

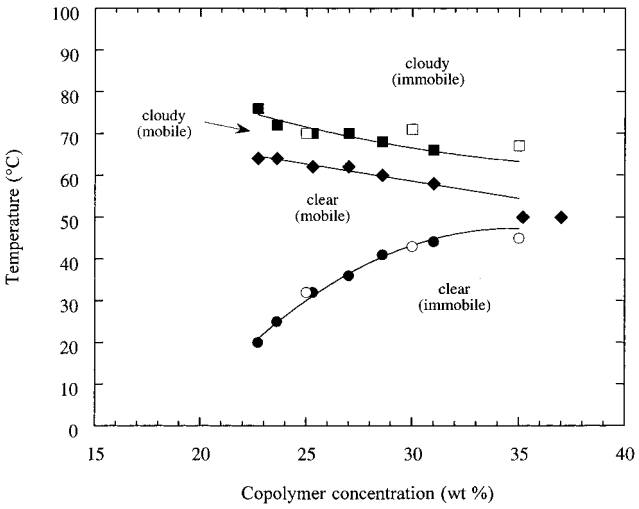

Figure 1. Phase diagram including transitions observed in the transparency and mobility of the $E_{40}B_{10}$ diblock copolymer gel (full symbols) by Deng *et al.*[1] and rheologically (open symbols), as a function of diblock copolymer concentration and temperature.

polyols (ICI plc). Aqueous solutions of these copolymers form cubic (spherical micelles), hexagonal (cylindrical micelles), and lamellar lyotropic liquid crystalline phases.[13−15] Under certain conditions, a bicontinuous spongelike L_3 phase can be formed.[14]

There is a measure of agreement that the low-temperature isotropic gel results from packing of the spherical micelles, irrespective of the copolymer type.[2−4,16−19] As the temperature of such a system is increased, the solvent becomes progressively poorer and a number of processes occur:

(i) The molecule−micelle equilibrium shifts further towards the micellar state.

(ii) The average number of molecules per micelle increases (Table 1).

(iii) The hard-sphere volume of the micelle, which determines the effective size for packing, initially increases as N increases but then decreases as the θ temperature of poly(oxyethylene) is approached (Table 1).

This latter process provides a mechanism for the release of packing constraints and the formation of a mobile fluid. Studies of the micellization and gelation of copolymer P85 ($E_{27}P_{39}E_{27}$) by Mortensen and co-workers[17,18] and Glatter *et al.*[19] provide a second mechanism for mobility at the high-temperature boundary, i.e., a transition from spherical to cylindrical micelles.

An interesting feature revealed by rheological measurements on micellar solutions of certain copolymers ($E_mP_nE_m$ and E_mB_n) is the formation of a complex fluid, referred to as a "soft gel",[11,15,20] and characterized either as a solution of cylindrical micelles of sufficient length to give relaxation times of the order of seconds (which gives an elastic response to an oscillatory stress)[20] or as a fractal network of spherical micelles.[11] By analogy with the results for the related copolymer $E_{41}B_8$,[11] all indications are that the mobile phases denoted in Figure 1 fit into this category.

In a previous study of block copolymer gels, Diat *et al.* employed a Couette cell to orient twinned face-centered cubic (fcc) crystals of a triblock copolymer solution at high shear rate and demonstrated, using small-angle X-ray scattering (SAXS), that high amplitude oscillatory shear ($\lambda = 40\%$) was able to anneal almost all of the defects.[21] Higgins and co-workers performed small-angle neutron scattering (SANS) experiments on a diblock copolymer in a selective solvent and observed ordered micellar phases for concentrations above 3 wt %.[22] The development of long-range order and subsequent melting at high shear rates was followed by performing SANS experiments on samples in a Couette cell.[22] It is also known that large-amplitude oscillatory shear in diblock copolymer melts leads to highly oriented structures. For example, highly oriented lamellar,[23] hexagonal (hex),[24] body-centered cubic (bcc),[25,26] and $Ia\bar{3}d$ (gyroid) phases[27,28] have all been prepared by the application of large-amplitude shear. The work presented here complements these earlier studies, comprising a systematic study of micellar ordering in gels of a low molecular weight diblock copolymer in which bcc, fcc, and hex micellar phases were accessed by variation of the polymer concentration and temperature.

The effects of large-amplitude oscillatory shear deformation of the samples were also studied in an attempt to prepare highly oriented samples and to study the effect of such deformation on the phase behavior. The identification of shear-induced structures was greatly facilitated by the employment of a novel X-ray rheometer which allowed confident association between the structural and orientational information yielded from the SAXS data and the dynamic mechanical properties determined from rheology.

Experimental Section

(1) Materials. The copolymer $E_{40}B_{10}$ used in the present work was a new preparation which, within the error of determination, was identical in its molecular characteristics with the sample used previously.[1] The chain length distribution of the sample was narrow: $M_w/M_n = 1.04$ determined by GPC based on poly(oxyethylene) calibrants and uncorrected for instrumental spreading. The materials used in this study were 23−38 wt % solutions of the copolymer in 0.2 mol dm^{-3} K_2SO_4, which were prepared by mixing at $T = 60-70$ °C, followed by several days storage in a refrigerator.

(2) Small-Angle X-ray Scattering. Simultaneous SAXS and rheology experiments were performed on either beam line 2.1 or 8.2 of the Synchrotron Radiation Source (SRS) at the Daresbury Laboratory, Warrington, U.K. Both beam lines are configured for SAXS experiments using monochromatic radiation of wavelength $\lambda = 1.5$ Å. Details of the storage ring, radiation, camera geometry, and data collection electronics have been given elsewhere.[29,30] Scattered photons were collected on a multiwire gas-filled area detector. Data were collected with a spatial resolution of 256 × 256 pixels over the active area of the detector.

A scattering pattern from an oriented specimen of wet collagen (rat tail tendon) was used for calibration of the q scale range of the detector, ($q = 4\pi \sin\theta/\lambda$, where the scattering angle is defined as 2θ). A parallel plate ionization detector placed before the sample cell recorded the incident intensity. The experimental data were corrected for background scattering (from the camera and empty shear cell), sample absorption, and positional alinearity of the detector.

(3) Rheometer. Rheological measurements were performed using a Rheometrics solids analyzer RSA II system with a shear sandwich geometry. The rheometer generates an oscillatory (sinusoidal) deformation, and the dynamic and loss shear moduli, respectively, G' and G'', are measured as a function of the deformation conditions. Available shear rates with this rheometer range between 10^{-3} and 10^2 s^{-1} with associated strains between 0.01 and 100%. Apertures were machined into the plates of the shear sandwich assembly to allow transmission of the X-ray beam, and were covered by Kapton windows of 6 μm thickness. The sample was loaded in two areas symmetrically about the insert piece, and the plates were machined precisely so that the area of the sample in contact with them measured 12 mm × 16 mm, (Figure 2). Sample thicknesses employed here were 0.5 mm: in general

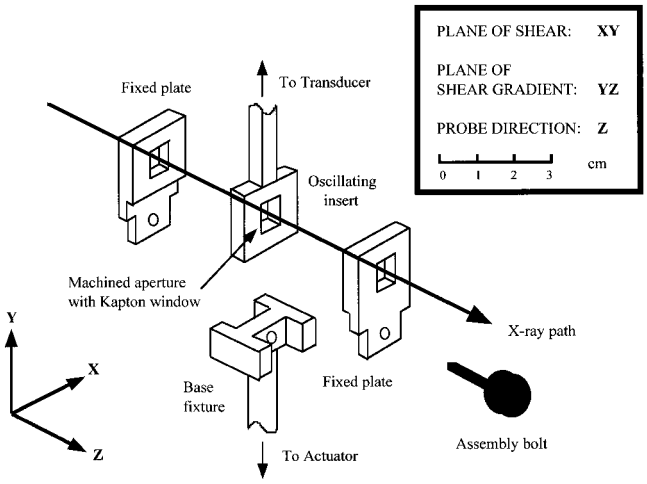

Figure 2. Shearing apparatus within the rheometer oven. The sample is loaded in a sandwich symmetrically about the central oscillating plate. All X-ray transmission apertures in the plates are covered with 6 μm Kapton windows.

this parameter is adjustable through the manufacture of insert pieces of differing thicknesses.

(4) Temperature Range. The sample is enclosed by an insulated oven that can be maintained at temperatures between −150 and 600 °C, controlled within an accuracy of ±1 °C. This oven was modified by the manufacturer with apertures in the surrounding insulation walls to allow transmission of the X-ray beam, which permitted the acquisition of SAXS patterns simultaneously with the rheological data during the deformation process. In these experiments, the samples were investigated at temperatures between −50 and 90 °C.

Water crystallized from the mixture at temperatures below −10 °C, forming a fine dispersion of ice crystals, followed by crystallization of a eutectic mixture at lower temperature. On raising the temperature, at a rate of 3 °C min^{-1}, diffraction rings characteristic of a hexagonal phase were seen in the SAXS pattern at $T \approx -10$ °C. This was assigned to the formation of a transient biphasic dispersion, comprising pure water and gel, with the gel having the high polymer concentration characteristic of the eutectic. Upon further heating above 0 °C, the dispersion rapidly homogenized to form a gel phase.

At higher temperatures, water began to evaporate from the solutions, thus affecting the concentration and phase behavior of the solutions. The phase behavior of the samples was reproducible upon heating and cooling for conditions where the sample was not exposed to temperatures above 85 °C, nor held significantly above room temperature for over 1 h. For these reasons, the results reported here are limited to the temperature range between 0 and 85 °C.

X-ray Rheology: Effect of Concentration and Temperature

Figure 3 shows the storage and loss moduli of the $E_{40}B_{10}$ gels as a function of the diblock copolymer concentration in the aqueous K_2SO_4 solvent. All data were collected at 25 °C with a frequency $\omega = 1$ s^{-1} and a strain amplitude of $\lambda = 0.1\%$ and were averaged from a series of five measurements. The viscoelastic behavior of these gels was linear for deformations up to $\lambda = 0.3\%$ strain amplitude, and thus the data shown in Figure 3 are within the linear viscoelastic regime. It can be seen from the figure that a higher concentration of copolymer within the gel leads to greater values of the shear moduli within this regime. Experiments measuring the dynamic shear moduli as a function of shear rate show a crossover between G' and G'' at a frequency of $\omega \approx 5$ rad s^{-1}, for a 25% $E_{40}B_{10}$ gel. This suggests that at a $\omega = 1$ rad s^{-1} the rheological response is sensitive to deformation of the micellar lattice.

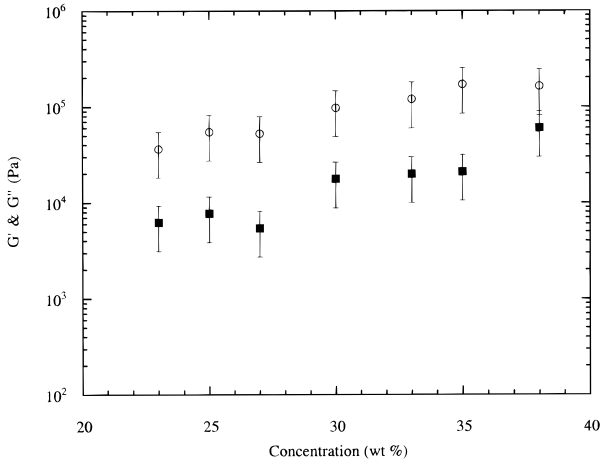

Figure 3. Storage modulus G' (open symbols) and loss modulus G'' (full symbols) as a function of $E_{40}B_{10}$ concentration in 0.2 mol dm^{-3} K_2SO_4. The samples are sheared at $\omega = 1$ rad s^{-1} with a strain amplitude of $\lambda = 0.1\%$, at a temperature of 25 °C.

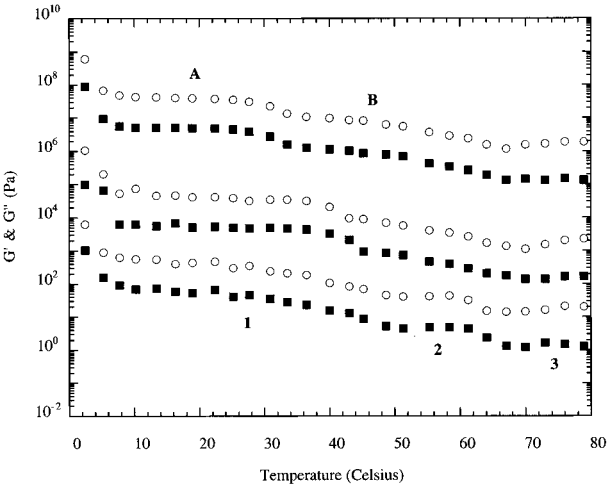

Figure 4. Storage modulus G' (open symbols) and loss modulus G'' (full symbols) as a function of sample temperature for three concentrations of $E_{40}B_{10}$ in 0.2 mold m^{-3} aqueous K_2SO_4: 25% (upper curve), 30% (central curve), and 38% (lower curve). The samples are sheared at $\omega = 1$ rad s^{-1} with a strain amplitude of $\lambda = 0.1\%$ and are heated at a rate of 3 °C min^{-1}. The notation correlates with the SAXS images shown in Figure 5. The upper and lower curves have been vertically displaced by a factor of 10^3 for clarity.

The storage and loss moduli of 25, 30, and 38% solutions of $E_{40}B_{10}$ as a function of temperature are shown in Figure 4. Again these data were collected at strain amplitudes of 0.1%, within the linear viscoelastic region. The integration time of the X-ray detection apparatus was set to 30 s, to match the data collection time of the rheometer. Thus, each two-dimensional X-ray image can be paired with a specific rheological measurement.

Two transitions can be seen in the dynamic shear moduli of the copolymer gels, characterized by a drop (typically of 1 order of magnitude) in both dynamic moduli. These transitions are marked in Figure 1 and show good agreement with existing observations of the mobility and transparency of the gel.[1]

The transitions in the rheological moduli are accompanied by changes in the sample structure, as revealed in the SAXS patterns. Samples with polymer concentrations of 30% or more showed an initial bcc phase at 5 °C (as characterized by a ratio between the positions of the first three diffraction rings of $1:2^{1/2}:3^{1/2}$,

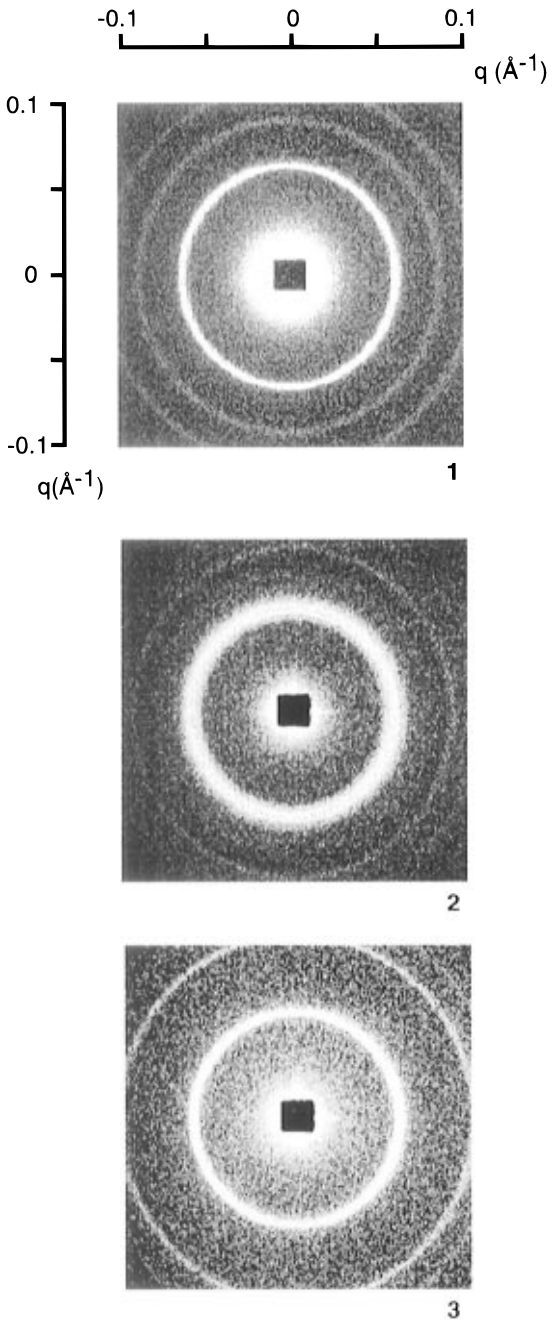

Figure 5. Three phases identified in 38% $E_{40}B_{10}$ diblock copolymer gel: (**1**) bcc structure between 5 and 50 °C; (2) fcc structure between 50 and 70 °C; and (3) hex structure between 70 and 80 °C. The images correlate with the numbered regions on the rheology data shown in Figure 4.

as shown in Figure 5 part 1) and, upon heating, two phase transitions before 85 °C. The first transition is from bcc to fcc, the latter having SAXS peaks in the positional ratio of $1(4/3)^{1/2}:(8/3)^{1/2}:(11/3)^{1/2}$,[31] (Figure 5 part 2). The second is from fcc to hex, with an observed ratio of $1:3^{1/2}:4^{1/2}$ between the peak positions of the first three diffraction rings (Figure 5 part 3). The temperatures at which these two transitions occur varied with polymer concentration: for the 33% $E_{40}B_{10}$ gel they occurred at approximately 35 and 68 °C, respectively, while for the higher concentration gels the phase transitions were observed at higher temperatures. We note that a region characterized by a single, broad peak was always observed between the fcc and hex phases: this is assigned to a biphasic region. The bcc phase was not observed for polymer concentrations below 30%. Instead, an fcc structure observed at room temperature

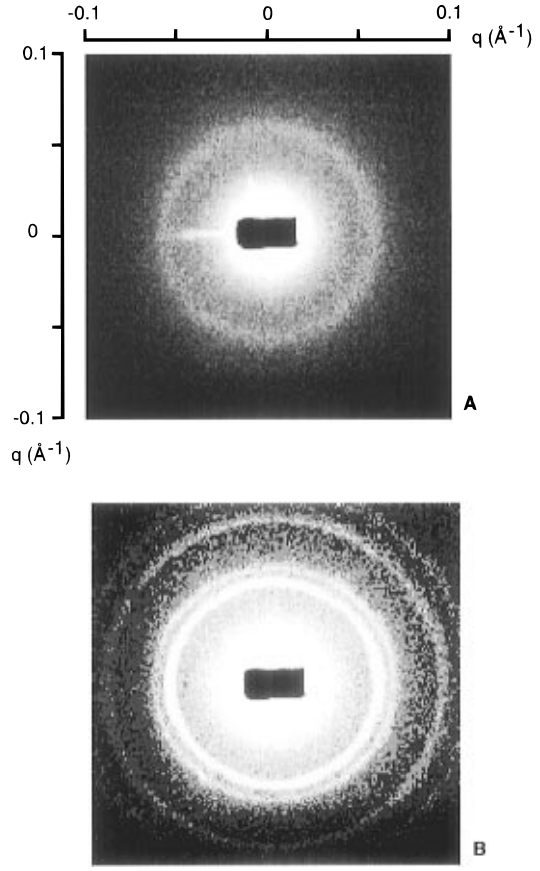

Figure 6. SAXS pattern showing the fcc structure observed between 30 and 60 °C in the 25% $E_{40}B_{10}$ diblock copolymer gel.

transformed, via a broad biphasic regime, to a hexagonal phase at high temperatures.

The fcc−hex transition seen in the SAXS data correlates with the high-temperature discontinuity in the rheological data (Figure 4) for all gel concentrations. In the case of the bcc−fcc transition for the higher concentration gels, (c > 30 wt %), the temperature of the SAXS transition correlates well with the temperature at which an inflection is seen in the dynamic moduli. For the lower concentration gels, a discontinuity in G' and G'' was observed at 30 °C. At temperatures below 30 °C, the SAXS patterns for the low-concentration gels showed only two diffraction rings: the first-order, (at q^*) and the third-order ring (at $(8/3)^{1/2}$ q^*), the latter being barely visible. At higher temperatures, the SAXS pattern contained all of the first four diffraction rings (Figure 6). It is noted that this transition occurred at the same temperature at which Deng *et al.* observed a mobile−immobile transition[1] (Figure 1). At this level of copolymer concentration, it is clear that this "soft gel" phase is formed from spherical micelles packed in an fcc lattice, and the mobility is believed to arise from many defects, i.e., islands of fcc-packed micelles in a continuum of a disordered phase, although the precise nature of the transitions in this region will be discussed more fully in a forthcoming paper.[32]

Combining transitions determined from SAXS and rheology, we find an overall phase diagram for these diblock copolymer gels as depicted in Figure 7. On heating from 5 °C, all samples form first a cubic phase and then a hex phase. The transition temperatures between the phases are concentration dependent, as indicated in the figure.

The observation of both fcc and bcc micellar phases in block copolymer solutions has been made before by

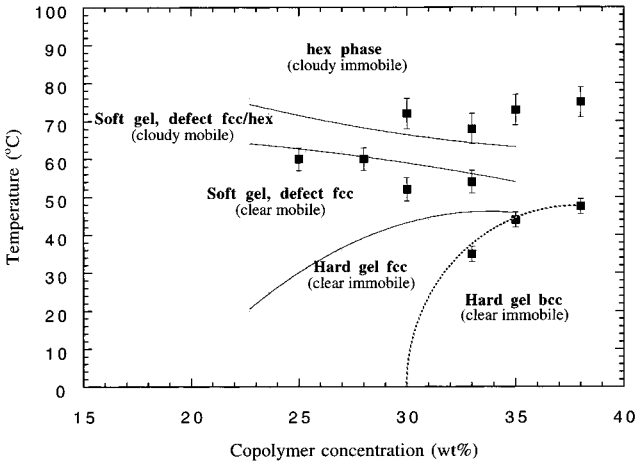

Figure 7. Phases observed by small-angle X-ray scattering in $E_{40}B_{10}$ diblock copolymer gels as a function of copolymer concentration and temperature. The full symbols mark the phase boundaries determined by SAXS, with the broken line as a guide to the eye, and the solid lines mark the mobility transitions determined by Deng *et al.*[1] The error bars indicate uncertainties associated with the phase transitions determined from repeated heating and cooling ramps.

other workers,[33,34] although a temperature-induced transition between the two has not been observed previously. Tiddy and co-workers performed extensive investigations on the phase behavior of poly(oxyethylene) alkyl ether surfactants (C_nEO_m) in aqueous solution and reported the observation of cubic and hexagonal micellar phases.[33] Gast and co-workers pointed out an analogy between their results[34] and Monte Carlo simulations on charged colloidal dispersions,[35,36] which indicates that an fcc phase is favored over a bcc phase as the intermicellar interactions become more short-ranged. In the work of Gast and co-workers, who studied PS−PI diblocks in solution in decane, the formation of either the fcc or bcc phase was rationalized by considering the ratio of the coronal layer thickness to the PS core radius. For relatively thin coronal layers, the intermicellar interactions are steeply repulsive, resulting in an fcc phase. As the corona becomes thicker, the interactions become softer and the bcc phase is stable. For our copolymers, the coronal layer contracts as the temperature rises, and more hydrophilic oxyethylene blocks are required to cover the surface of the micelle, resulting in an increase in association number[1] and micellar core radius, as has also been seen in oxyethylene−oxypropylene−oxyethylene triblock systems.[37,38] Thus, the phase transition from bcc to fcc with increasing temperature also yields an increase in packing fraction from 0.68 in the bcc phase to 0.74 in the fcc phase.

A novel aspect of the results presented here is the observation of both fcc and bcc phases in the same block copolymer solution as a function of temperature. The observation that the bcc phase window widens with increasing volume fraction of polymer (Figure 7) is consistent with intermicellar interactions becoming more like those of "soft spheres", leading to a bcc phase, which is the phase observed for block copolymer melts. Theory for block copolymer melts suggests that the free energy difference between bcc, fcc, and hex micellar phases is very small in the absence of solvent: indeed, a sequence of transitions between these structures is predicted near the ODT.[39]

Our observations correlate well with those of Gast and co-workers,[34] except that temperature plays an important role in changing solvent quality in our system.

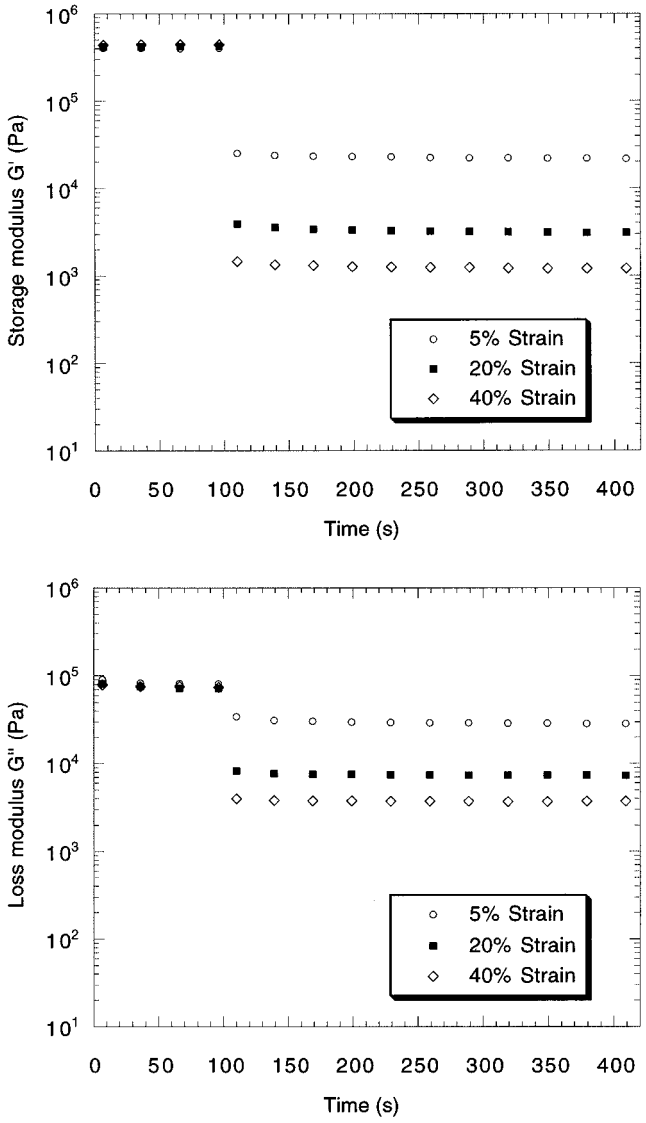

Figure 8. Dynamic shear moduli of 35% $E_{40}B_{10}$ diblock copolymer gel sheared at 25 °C with a frequency of $\omega = 1$ s^{-1} and a strain amplitude of $\lambda = 0.1\%$ for 2 min and then over larger amplitudes (as indicated) for 5 min.

Specifically, as the temperature is increased the micellar fringe contracts (negative temperature coefficient of solubility), while the core becomes bigger, as seen in the increasing values of N_w, (Table 1). Hence the steric repulsive energy operates over a shorter range. This results in a phase transition from bcc to fcc (Figure 7), as a function of temperature in our system, whereas a bcc−fcc transition was not reported by Gast and co-workers.[34]

X-ray Rheology: Effect of Large-Amplitude Reciprocating Shear

The effect of shearing at amplitudes greater than that which defines the linear viscoelastic region was investigated by dynamic experiments performed on the 35% gel, the results of which are shown in Figure 8. In each experiment the gel was subjected to an oscillatory shear deformation of a frequency of 1 rad s^{-1} and an amplitude of 0.1% for 2 min, after which the shear amplitude was discontinuously incremented to increasingly greater values, as detailed in the figure, at the same shear rate.

Upon application of a large-amplitude shear, a rapid (i.e., within the 30 s temporal resolution) decrease was observed in the values of the dynamic moduli, which remained at new, constant values for the remaining 5

min of each experiment. Larger nonlinear shear amplitudes resulted in larger decreases in the shear moduli. We note that G' and G'' are not rigorously defined in the nonlinear viscoelastic regime at large strain amplitudes. However, they are quantities that can be extracted from our rheometer which indicate the extent of shear thinning that occurs in these gels.[40]

During the application of large-amplitude reciprocating shear in the rheometer, SAXS data were acquired simultaneously. Again the temporal resolution of the rheology measurements was set to 30 s, in order to match that of the integration time of the SAXS acquisition. The experiments performed had five common stages. In stage 1 the sample was sheared at 1 s^{-1} at an amplitude of $\lambda = 0.1\%$ for 5 min; in stages 2−4 the sample was sheared with a strain of 50% for shear rates 0.1, 1, and 10 rad s^{-1}, respectively. The duration of stage 2 was 10 min, while stages 3 and 4 lasted 5 min each: this provided a minimum deformation for each stage of 30 shear units. Here the deformation unit τ is the dimensionless quantity defined as

$$\tau = |\lambda|\dot{\gamma}t \qquad (1)$$

for a shear deformation of amplitude λ, shear rate $\dot{\gamma}$ and duration time t. Finally in stage 5, the shear was reduced to the same level as stage 1 for 20 min, in order to observe any relaxation effects following the nonlinear deformations. This experimental sequence was performed on seven concentrations of $E_{40}B_{10}$ gels: 23, 25, 28, 30, 33, 35, and 38%. All experiments were performed at 25 °C, and therefore, the lower four concentration gels were sheared in the fcc phase, and the three higher concentration gels were sheared in the bcc phase (Figure 7). As an example of the results obtained, the dynamic shear moduli and SAXS patterns from the 30% $E_{40}B_{10}$ gel are illustrated in Figure 9.

It is apparent from the SAXS pattern that the 30% $E_{40}B_{10}$ sample was partially oriented in the initial state, revealing the presence of six equally spaced intensity maxima on the first-order diffraction ring (Figure 9b, part 1). This orientation arose from the shear deformation that occurred during the cell loading procedure. This pattern can be interpreted using a model of a defected fcc structure, as illustrated in Figures 10 and 11. Diffraction occurs from several types of grain, corresponding to distinct orientations of the structure.

Figure 10 shows the unit cell of the fcc structure and the projection of the (111) and (200) planes. Diffraction from the (200) planes gives rise to the four azimuthal maxima evident in the outer diffraction ring (Figure 9b). We propose that the six equispaced azimuthal maxima evident on the inner diffraction ring arise from finite ABCABC... stacking sequences of (111) planes of the fcc structure. In particular, it is likely that the actual stacking arrangement involves a combination of ABCABC... (fcc) packing and ABAB... (hexagonal close packed (hcp)) sequences. This is consistent with the fact that the critical packing fraction, 0.74, is the same for the fcc and hcp phases and the observation that these two structures may be nearly degenerate in free energy.[39,41] That a hexagon of reflections can be modelled as a combination of hcp and fcc packing has been suggested previously by Gast and co-workers.[42] The result is a broadening of the Bragg diffraction spots to Bragg rods (Figure 11) and the resulting intersection with the (111) plane in reciprocal space containing $q = 0$ produces the hexagonally arranged scattering maxima observed in the diffraction plane, (Figure 9b).

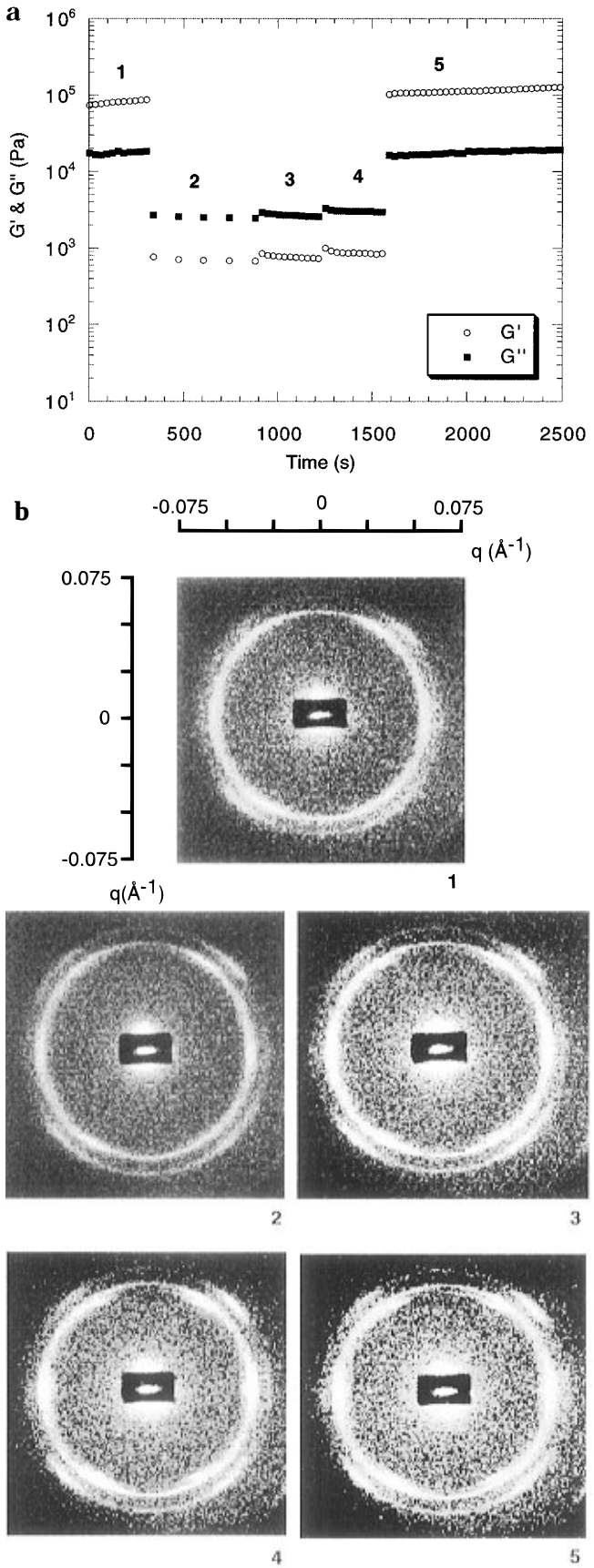

Figure 9. (a) Dynamic shear moduli G'(○) and G''(■) and (b) SAXS data collected for a five-stage dynamic shear experiment performed on a 30% $E_{40}B_{10}$ diblock copolymer gel at 25 °C: (1) $\omega = 1$ rad s^{-1}, $\lambda = 0.1\%$; (2) $\omega = 0.1$ rad s^{-1}, $\lambda = 50\%$; (3) $\omega = 1$ rad s^{-1}, $\lambda = 50\%$; (4) $\omega = 10$ rad s^{-1}, $\lambda = 50\%$; (5) $\omega = 1$ rad s^{-1}, $\lambda = 0.1\%$. Measurements of G' and G'' were made every 30 s, which was also the integration time for the X-ray images. Each X-ray image shown was taken coincidentally with the last rheological measurement of each respective stage.

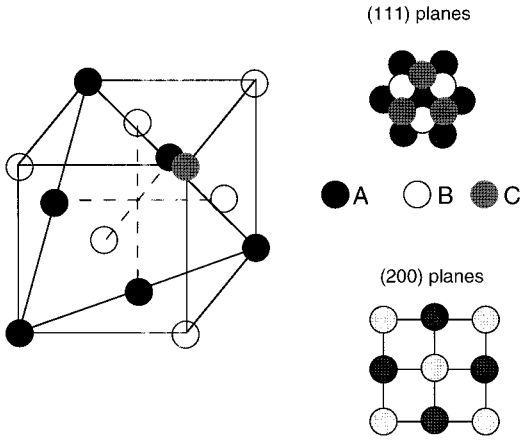

Figure 10. Representation of the unit cell for the fcc phase (left) and the projections of the (111) and (200) planes (right).

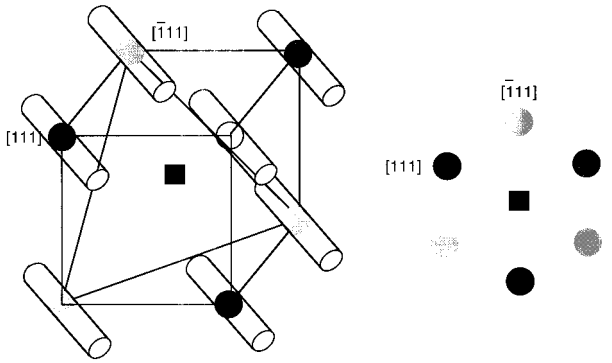

Figure 11. Schematic depiction of the broadening of the Bragg reflections in the fcc phase into Bragg rods due to finite sequences of ABCABC... stacking interspersed with ABAB... stacking (left). The intersections of the [111] and [$\bar{1}$11] Bragg rods with the $q = 0$ plane in reciprocal space give the observed hexagonal symmetry for the inner peaks in Figure 9b.

The relaxation behavior following large-amplitude shear was found to be quite different in the rheological and X-ray data. The rheological data of Figure 9a indicate that large-amplitude shearing causes an effect within the gel that is independent of the rate of applied shear, as neither G' nor G'' altered as the shear rate was increased by two orders of magnitude. (Of course, Figure 8 demonstrates that the moduli are sensitive to changes in the amplitude of the applied deformation.) In contrast, the SAXS images (Figure 9b parts 2−4) changed as the shear rate was incremented, suggesting a higher degree of orientational order. It is noted that each SAXS pattern displayed in Figure 9b is considered to be representative of the steady state condition, as they remained unchanged for the last few minutes of each sequence. The two data sets also reveal contrasting information upon cessation of shear: the rheological data show that total recovery to the initial condition occurred, while the SAXS data show that, over the same time scale, there was not a return to the initial pattern.

The observed effects may be understood in terms of a polydomain structure within the gel. We suggest that the effect of large-amplitude shear is twofold: to increase the defect density within the polydomain structure, in contrast to the observations of Diat *et al.* from SAXS experiments on a sheared triblock copolymer gel,[21] and also to increase the orientation of domains with respect to the common axis of the shear direction. The shear rate has been demonstrated to be the dominant factor in the determination of the degree of orientation of domains within polymer systems[43,44] and is therefore considered to do so here also, while the shear amplitude may well play the dominant role in the multiplication of defects. It should also be noted that the SAXS scattering patterns correspond to an average of the structure, over the illuminated portion of the sample, while the measurements of the rheological moduli will be highly sensitive to local defect density.

Thus, the results recorded in Figure 9 are understood as comprising a discontinuous increase in defect density between stages 1 and 2 which produces a discontinuous change in the rheological moduli. Nevertheless the shear rate associated with stage 2 is small, and therefore the induced global orientation is slight. As the shear rate is increased (stages 2−4), with the amplitude held fixed (hence G' and G'' remain constant), the global orientation of the sample steadily increases as more domains are aligned to the shear direction. This is evidenced in the SAXS data by the sharpening of the six azimuthal maxima on the inner diffraction ring. Upon cessation of shear, the defect structure anneals away rapidly, resulting in a rapid recovery of the initial values of the rheological moduli, while the orientation of the aligned domains remains unaltered, resulting in the final SAXS pattern remaining the same as the last pattern from the sheared gel (at least over a time scale of 20 min), in agreement with the data shown in Figure 9. This reasoning agrees with the conclusions of Higgins and co-workers, who, in their oscillatory shear study of a diblock copolymer of polystyrene-*b*-(ethylene-*co*-propylene) in dodecane, concluded that the evidence from SANS and rheological measurements was consistent with a picture where upon cessation of shear short-range order was quickly restored, but long-range order was very slow to reappear.[45]

Conclusions

Diblock copolymer gels of $E_{40}B_{10}$ in 0.2 mol dm^{-3} aqueous K_2SO_4 have been shown to display a rich variety of ordered phases. A body-centered cubic structure, a face-centered cubic structure, and a hexagonally packed rod phase are all observed depending on gel concentration and temperature. Gels with more than 30% diblock exhibit a bcc phase at low temperatures which changes to an fcc phase as the temperature is increased. Our observations, the theoretical and experimental observations of Gast and co-workers,[34,36,42] and measurements of micelle structure by light scattering[1] enable us to conclude that this is due to a temperature-induced thinning of the coronal layer. The decrease in coronal thickness of the micelle results in intermicellar interactions of shorter range, and, thus, increasingly favours the fcc structure as the temperature rises. We find that the transition temperature between the bcc and fcc phases is highly concentration dependent: increasing in the case of higher concentration, broadening the temperature range over which the bcc phase exists.

The application of large-amplitude ($\lambda = 50\%$) oscillatory shear to the gels results in changes to both the dynamic shear moduli and the small-angle X-ray scattering pattern. The storage modulus is reduced, typically by 2 orders of magnitude, by the application of shear, as is the loss modulus, although to a lesser extent. The SAXS patterns obtained simultaneously show a sharpening of the diffraction rings, indicating an increase in the degree of order. Our interpretation is that these two shear-induced effects do not arise from the same source. The rheological measurements are sensitive to the defect density, which is increased by an increase in the amplitude of shear. The SAXS patterns

reveal the global orientation of the polymer gel domains, which is increased by an increase in the shear rate.

Upon cessation of shear, many defects are annihilated but the oriented domains retain their degree of alignment to the shear direction. The dynamic shear moduli G' and G'' therefore return to their initial values but the SAXS pattern does not reveal any relaxation effects, within the timescale of our experiments. The global shear-induced structure either is trapped, or only relaxes very slowly.[32,45] These results highlight the value of simultaneous SAXS and rheology measurements, because changes in the dynamic mechanical properties can be correlated directly to structural changes determined via SAXS.

Acknowledgment. The authors are grateful to the Engineering and Physical Sciences Research Council (U.K.) for the awards of grants (GR/K03982, GR/K56117, and GR/J25994) which supported this work. The CLRC is acknowledged for the provision of beam time at Daresbury.

References and Notes

(1) Deng, N.-J.; Luo, Y. Z.; Tanodekaew, S.; Bingham, N.; Attwood, D.; Booth, C. *J. Polym. Sci. B* **1995**, *33*, 1085.
(2) Bedells, A. D.; Arafeh, R. M.; Yang, Z.; Attwood, D.; Heatley, F.; Padget, J. C.; Price, C.; Booth, C. *J. Chem. Soc., Faraday Trans* **1993**, *89*, 1235.
(3) Bedells, A. D.; Arafeh, R. M.; Yang, Z.; Attwood, D.; Padget, J. C.; Price, C.; Booth, C. *J. Chem. Soc., Faraday Trans.* **1993**, *89*, 1243.
(4) Tanodekaew, S.; Deng, N.-J.; Smith, S.; Yang, Y. W.; Attwood, D.; Booth, C. *J. Phys. Chem.* **1993**, *97*, 11847.
(5) Yang, Z.; Pickard, S.; Deng, N.-J.; Barlow, R. J.; Attwood, D.; Booth, C. *Macromolecules* **1994**, *27*, 2371.
(6) Yang, Y.-W.; Deng, N.-J.; Yu, G.-E.; Zhou, Z.-K.; Attwood, D.; Booth, C. *Langmuir* **1995**, *11*, 4703.
(7) Yu, G.-E.; Yang, Y.-W.; Yang, Z.; Attwood, D.; Booth, C.; Nace, V. M. *Langmuir* **1996**, *12*, 3404.
(8) Bailey, F. E.; Callard, R. W. *J. Appl. Polym. Sci.* **1959**, *1*, 373.
(9) Beech, D. R.; Booth, C. *J. Polym. Sci., Part A2.* **1969**, *7*, 575.
(10) Godward, J.; Heatley, F.; Smith, S.; Tandekaew, S.; Yang, Y.-W.; Booth, C. *J. Chem. Soc., Faraday Trans.* **1995**, *91*, 3461.
(11) Li, H.; Yu, G.-E.; Price, C.; Booth, C.; Hecht, E.; Hoffmann, H. *Macromolecules* **1997**, *30*, 1347.
(12) Yang, Y.-W.; Ali-Adib, Z.; McKeown, N. B.; Ryan, A. J.; Attwood, D.; Booth, C. *Langmuir* **1997**, *13*, 1860.
(13) Wanka, G.; Hoffmann, H.; Ulbricht, W. *Macromolecules* **1994**, *27*, 4145.
(14) Hecht, E.; Mortensen, K.; Hoffmann, H. *Macromolecules* **1995**, *28*, 5465.
(15) Almgren, M.; Brown, W.; Hvidt, S. *Colloid Polym. Sci.* **1995**, *273*, 2.
(16) Yu, G.-E.; Deng, Y.-L.; Dalton, S.; Wang, Q.-G.; Attwood, D.; Price, C.; Booth, C. *J. Chem. Soc., Faraday Trans.* **1992**, *88*, 2537.
(17) Mortensen, K.; Pedersen, J. S. *Macromolecules* **1993**, *26*, 805.
(18) Mortensen, K. *Europhys. Lett.* **1992**, *19*, 599.
(19) Glatter, O.; Scherf, O.; Schillén, K.; Brown, W. *Macromolecules* **1994**, *27*, 6046.
(20) Hvidt, S.; Jorgensen, E. B.; Brown, W.; Schillén, K. *J. Phys. Chem.* **1994**, *98*, 12320.
(21) Diat, O.; Porte, G.; Berret, J.-F. *Phys. Rev. B* **1996**, *54*, 14869.
(22) Phoon, C. L.; Higgins, J. S.; Allegra, G.; Van Leeuwen, P.; Staples, E. *Proc. R. Soc. London A* **1993**, *442*, 221.
(23) Koppi, K. A.; Tirrell, M.; Bates, F. S.; Almdal, K.; Colby, R . H. *J. Phys. II Fr.* **1992**, *2*, 1941.
(24) Tepe, T.; Schulz, M. F.; Zhao, J.; Tirrell, M.; Bates, F. S.; Mortensen, K.; Almdal, K. *Macromolecules* **1995**, *28*, 3008.
(25) Koppi, K. A.; Tirrell, M.; Bates, F. S.; Almdal, K.; Mortensen, K. *J. Rheol.* **1994**, *38*, 999.
(26) Almdal, K.; Koppi, K. A.; Bates, F. S. *Macromolecules* **1993**, *26*, 4058.
(27) Khandpur, A. K.; Förster, S.; Bates, F. S.; Hamley, I. W.; Bras, W.; Almdal, K.; Mortensen, K. *Macromolecules* **1995**, *28*, 8796.
(28) Förster, S.; Khandpur, A. K.; Zhao, J.; Bates, F. S.; Hamley, I. W.; Ryan, A. J.; Bras, W. *Macromolecules* **1994**, *27*, 6922.
(29) Towns-Andrews, E.; Berry, A.; Bordas, J.; Mant, G. R.; Murray, P. K.; Roberts, K.; Sumner, I.; Worgan, J. S.; Lewis, R.; Gabriel, A. *Rev. Sci. Instrum.* **1989**, *60*, 2346.
(30) Bras, W.; Derbyshire, G. E.; Ryan, A. J.; Mant, G. R.; Felton, A.; Lewis, R. A.; Hall, C. J.; Greaves, G. N. *Nucl. Instrum. Methods Phys. Res.* **1993**, *A326*, 587.
(31) It is noted that this sequence of reflections can be obtained from the $Ia\bar{3}d$ cubic phase; nevertheless, considering the absence of the $(14/3)^{1/2}$ reflection that would be anticipated from this phase, and the overwhelming evidence from light scattering experiments,[1] we conclude that the structure is a micellar fcc (space group $Fm\bar{3}m$) phase.
(32) Hamley, I. W.; Pople, J. A.; Fairclough, J. P. A.; Ryan, A. J.; Yu., G.-E.; Booth, C. in preparation.
(33) Mitchell, D. J.; Tiddy, G. J. T.; Waring, L.; Bostock, T.; McDonald, M. P. *J. Chem. Soc., Faraday Trans. 1* **1983**, *79*, 975.
(34) McConnell, G. A.; Gast, A.; Huang, J. S.; Smith, S. D. *Phys. Rev. Lett.* **1993**, *71*, 2102.
(35) Robbins, M. O.; Kremer, K.; Grest, G. S. *J. Chem. Phys.* **1988**, *88*, 3286.
(36) Monovoukas, Y.; Gast, A. P. *J. Colloid Interface Sci.* **1989**, *128*, 533.
(37) Jørgensen, E. B.; Hvidt, S.; Brown, W.; Schillén, K. *Macromolecules* **1997**, *30*, 2355.
(38) Chu, B.; Zhou, Z. in *Nonionic Surfactants: Polyoxyalkylene Block Copolymers*; Nace, V. N., Ed.; Marcel Dekker: New York, 1996.
(39) Semenov, A. N. *Macromolecules* **1989**, *22*, 2849.
(40) Macosko, C. W. *Rheology: Principles, Measurements and Applications*; VCH: New York, **1994**.
(41) Matsen, M. W.; Bates, F. S. *Macromolecules* **1996**, *29*, 1091.
(42) McConnell, G. A.; Lin, M. Y.; Gast, A. P. *Macromolecules* **1995**, *28*, 6754.
(43) Pople, J. A.; Mitchell, G. R.; Chai, C. K. *Polymer* **1996**, *37*, 4187.
(44) Gervat, L.; Mackley, M. R.; Nicholson, T. M.; Windle, A H. *Philos. Trans. R. Soc. London A.* **1995**, *350*, 1.
(45) Higgins, J. S.; Blake, S.; Tomlins, P. E.; Ross-Murphy, S. B.; Staples, E.; Penfold, J.; Dawkins, J. V. *Polymer* **1988**, *29*, 1968.

MA970308J